European Review for Medical and Pharmacological Sciences 2019; 23: 9574-9581

MiR-135a inhibitor alleviates pulmonary arterial hypertension through β-Catenin/GSK-3β signaling pathway

R.-H. YU[1], L.-M. WANG[1], X.-H. HU[2]

[1]Department of Respiratory Medicine, Xuhui District Central Hospital, Shanghai, China
[2]Department of Critical Care Medicine, Xuhui District Central Hospital, Shanghai, China

Abstract. – OBJECTIVE: The aim of this study was to investigate the regulatory role of micro-ribonucleic acid (miR)-135a in monocrotaline (MCT)-induced pulmonary arterial hypertension (PAH) in rats, and to analyze the possible regulatory mechanism.

MATERIALS AND METHODS: A total of 30 Sprague-Dawley rats were randomly divided into three groups, including the blank control group, model group and miR-135a inhibitor intervention group. The right ventricular systolic pressure (RVSP) and right ventricle hypertrophy index (RVHI) were measured in rats of each group. Hematoxylin and eosin (HE) staining was adopted to detect the pathological changes in lung tissues of rats. Enzyme-linked immunosorbent assay (ELISA) was performed to measure the levels of interleukin-6 (IL-6) and IL-1β in lung tissues. Meanwhile, the messenger RNA (mRNA) and protein levels of β-catenin and glycogen synthase kinase-3β (GSK-3β) in lung tissues of rats were determined via Reverse Transcription-Polymerase Chain Reaction (RT-PCR) and Western blotting assay, respectively.

RESULTS: Compared with the blank control group, RVSP and RVHI increased significantly in the model group. The pathological morphology of the lung tissues was poor, and the content of IL-6 and IL-1β was markedly up-regulated in the model group. Meanwhile, the mRNA and protein levels of β-catenin and GSK-3β were notably elevated in the model group than the blank control group. In the miR-135a inhibitor intervention group, RVSP and RVHI decreased significantly, and the pathological morphology of lung tissues was evidently improved when compared with the blank control group. Furthermore, the content of IL-6 and IL-1β was remarkably reduced, and the mRNA and protein levels of β-catenin and GSK-3β were significantly declined in the miR-135a inhibitor intervention group.

CONCLUSIONS: MiR-135a inhibitor significantly alleviates inflammatory response in the lung tissues and ameliorates damage to the pathological morphology. The possible underlying mechanism may be associated with the β-catenin/GSK-3β signaling pathway.

Key Words:
MiR-135a, Pulmonary arterial hypertension (PAH), β-catenin, GSK-3β, Inflammatory response.

Introduction

Pulmonary arterial hypertension (PAH) is a severe disease characterized by a progressive increase in pulmonary vascular resistance and artery pressure caused by pulmonary artery occlusion. Meanwhile, PAH is accompanied by irreversible pulmonary vascular remodeling, eventually resulting in right heart failure related death[1,2]. The characteristics of PAH include increased pulmonary vascular resistance, pulmonary vascular endothelial dysfunction and aggravated thrombosis and inflammatory response. However, the pathogenesis of PAH is complex and remains unknown. Major theories of PAH pathogenesis include abnormal proliferation and differentiation of pulmonary artery smooth muscle cells and endothelial cells, as well as excessive proliferation and migration of pulmonary vascular fibroblasts[3,4]. In recent years, researchers have paid more and more attention to the important role of abnormal proliferation of pulmonary artery smooth muscle cells in the pathogenesis of PAH. Under normal physiological conditions, pulmonary artery smooth muscle cells are quiescent in organisms. However, they are in a state of abnormal proliferation in patients with PAH[5].

The β-catenin/glycogen synthase kinase-3β (GSK-3β) signaling pathway is a vital signaling pathway in the Wnt family. When stimulated, the Wnt protein can penetrate the cell membrane, activate downstream signals in the cytoplasm and promote the GSK-3β compound to detach from

Corresponding Author: Xinhua Hu, BM; e-mail: xhyyhxh@163.com

the complex. This may eventually trigger the disturbance of β-catenin ubiquitination and lead to massive β-catenin deposition in the cytoplasm[6,7]. Acting as a downstream target of β-catenin, GSK-3β widely existed in cells. Meanwhile, it regulates multiple biological processes, such as cell survival, proliferation, differentiation and apoptosis[8]. Bahrami et al[9] have indicated that GSK-3β plays a crucial role in the growth, development and senescence of living individuals.

Microribonucleic acids (miRNAs) are a category of highly conserved non-coding single-stranded RNAs with 20-25 nucleotides in length. MiRNAs mainly promote the degradation of target genes or inhibit their translation into proteins. A large number of researches have found that miRNAs participate in the occurrence and development of PAH[10]. Currently, studies have demonstrated that miR-135a is significantly up-regulated in PAH patients. However, its mechanism of regulating PAH has not been fully elucidated. In this paper, a rat model of PAH was successfully established *via* intraperitoneal injection of monocrotaline (MCT). The aim of this study was to investigate the role of miR-135a inhibitor in PAH, and to explore the regulatory mechanism.

Materials and Methods

Laboratory Animals

Sprague-Dawley rats used in this experiment were purchased from the Laboratory Animal Center of Sun Yat-Sen University. All rats were fed under the conditions of 12/12 h light/dark cycle and constant temperature of (22±2)°C. Meanwhile, the rats were given free access to water and food. This study was approved by the Animal Ethics Committee of Xuhui District Central Hospital Animal Center.

Experimental Reagents

MCT (Sigma-Aldrich, St. Louis, MO, USA), β-catenin, GSK-3β and β-actin antibodies (Cell Signaling Technology, Danvers, MA, USA), Horseradish Peroxidase (HRP)-labeled secondary antibodies (Beijing Bioss Biological Technology Co., Ltd., Beijing, China), 4% paraformaldehyde and diaminobenzidine (DAB) developer (Beijing Solarbio Science & Technology Co., Ltd., Beijing, China), interleukin-6 (IL-6) and IL-1β kits (Abcam, Cambridge, MA, USA), and β-catenin and GSK-3β primers (Thermo Fisher Scientific, Waltham, MA, USA).

Experimental Instruments

PowerLab Biological Signal Collection and Processing System was purchased from ADInstruments (Bella Vista, NSW, Australia), Polymerase Chain Reaction (PCR) instrument from Hangzhou LongGene Scientific Instruments Co., Ltd. (Hangzhou, China), and microplate reader from Thermo Fisher Scientific (Waltham, MA, USA).

Establishment of Rat Model of PAH

A total of 30 rats were randomly divided into three groups, including the blank control group, model group and miR-135a inhibitor intervention group. The symptoms of PAH model established through the injection of monocrotaline, a kind of alkaloid, were the most similar to those of human idiopathic PAH. In this experiment, MCT (60 mg/kg) was injected intraperitoneally to establish the rat model of PAH in the model group and miR-135a inhibitor intervention group. 14 d later, the modeling status was observed among the rats. Meanwhile, rats in the blank control group were intraperitoneally injected with normal saline as controls.

Measurement of Right Ventricular Systolic Pressure (RVSP) and Right Ventricle Hypertrophy Index (RVHI)

The rats in each group were intraperitoneally injected with pentobarbital sodium (40 mg/kg). After anesthesia, an incision was made on the neck. The right external jugular vein was dissected using a blunt separator. After ligating the distal end of the external jugular vein, the proximal end was cut open. Subsequently, a PE-50 catheter was gently inserted, with the other end connected to a pressure converter. The position of the catheter was determined according to the changes in pressure value and pressure curve displayed on the screen. The catheter was then fixed after the pulmonary arterial pressure waveform occurred. RVSP was recorded using the PowerLab Biological Signal Collection and Processing System. After that, the catheter was withdrawn, and the right external jugular vein was ligated. Next, the heart was separated. The ventricle was cut into two parts, namely right ventricular free wall (RV) and left ventricle + septum (LV+S), followed by weighing separately. The ratio of RV to LV+S was calculated as RVHI [RVHI = RV/(LV+S)][11].

Detection of Changes in Pathological Morphology of Rat Lung Tissues via Hematoxylin and Eosin (HE) Staining

The lung tissues of rats in each group were dissected and soaked in paraformaldehyde for fixation. Then, the tissues were dehydrated in 80% ethanol and embedded in paraffin. After being sliced into sections and deparaffinized with xylene, the sections were dehydrated in a gradient of ethanol. Next, the sections were stained with hematoxylin and eosin for 1 min, respectively, followed by washing with Phosphate-Buffered Saline (PBS; Gibco, Grand Island, NY, USA) 3 times (5 min each). Finally, the tissues were mounted in neutral resin and observed under a microscope.

Detection of IL-6 and IL-1β Levels in Rat Lung Tissues via Enzyme-Linked Immunosorbent Assay (ELISA)

The lung tissues of rats were extracted, ground and centrifuged. Then, the supernatant was collected. According to the instructions of ELISA kit (R&D Systems, Minneapolis, MN, USA), 100 μL Assay Diluent RD1W solution was added into each well, followed by addition of 100 μL standard substance and sample for 2 h of incubation at room temperature. Subsequently, the solution was absorbed, and 200 μL Substrate Solution was added for 20 min of incubation. 50 μL stop buffer was added to terminate the reaction. Finally, the absorbance at λ =450 nm was measured.

Detection of Messenger RNA (mRNA) Levels of β-Catenin and GSK-3β in Rat Lung Tissues via Reverse Transcription (RT)-PCR

Total RNA was extracted from lung tissues of rats in each group using the TRIzol reagent (Invitrogen, Carlsbad, CA, USA). After the addition of chloroform and isopropyl alcohol, the tissues were centrifuged and the supernatant was collected. The concentration of extracted RNA was measured. Subsequently, RNA sample was reversely transcribed into complementary deoxyribose nucleic acid (cDNA) according to the instructions of the RT kit. Specific Polymerase Chain Reaction (PCR) amplification was performed as follows: annealing at 58°C for 35 cycles. After that, 1% agarose gel electrophoresis was conducted. Primer sequences used in this study were as follows: β-catenin, F: 5'-CAAGCGAATCCTCACACGC-3', R: 5'-GCTACGGACGTATCCGGAGCC-3'; GSK-3β, F: 5'-ATGCCAAGTGGCAGGATAA-3', R: 5'-GCGAGCGACTACCTCAGTACT-3'; β-actin: F: 5'-CCTGGCACCCAGCACAAT-3', R: 5'-GCTGATCCACATCTGCTGGAA-3'.

Detection of Protein Levels of β-Catenin and GSK-3β in Rat Lung Tissues via Western Blotting Assay

Total proteins in lung tissues of rats in each group were extracted. The tissues were lysed using lysis buffer (Beyotime, Shanghai, China), followed by centrifugation and collection of the supernatant. The concentration of extracted protein was determined by the Bradford method. Subsequently, extracted protein samples were separated by 10% sodium dodecyl sulphate-polyacrylamide gel electrophoresis (SDS-PAGE) and transferred onto polyvinylidene difluoride (PVDF) membranes (Millipore, Billerica, MA, USA) at 25 V for 2.5 h. After sealing with 5% bovine serum albumin (BSA), the membranes were washed with Tris-Buffered Saline and Tween 20 (TBST, Sigma-Aldrich, St. Louis, MO, USA) for 5 min and incubated with primary antibodies at 4°C overnight. On the next day, the membranes were incubated with secondary antibodies at room temperature for 1 h. Color development was performed with diaminobenzidine (DAB; Solarbio, Beijing, China) developer. The optical density of immune-reactive bands was analyzed using Image J software (NIH, Bethesda, MD, USA). β-actin was used as an internal control.

Statistical Analysis

Statistical Product and Service Solutions (SPSS) 17.0 software (SPSS Inc., Chicago, IL, USA) was adopted for all statistical analysis. Experimental data were presented as mean ± standard deviation. One-way analysis of variance (ANOVA) was used to compare the differences among different groups, followed by Post-Hoc Test (Least Significant Difference). $p<0.05$ was considered statistically significant.

Results

Establishment of PAH Model in Rats

7 d after injection, the body weight, activity amount and food intake decreased significantly in the rat model of PAH. As for modeling by MCT injection, it has been reported that an ideal PAH model can be established within about 14 d. After the rats were sacrificed, the lung surface

was smooth and off-white, with poor elasticity. Meanwhile, the right ventricle was thickened. According to the measurement of pulmonary artery pressure *via* PowerLab Biological Signal Collection and Processing System, pulmonary artery pressure value >25 mmHg indicated the successful establishment of PAH model in rats. Subsequently, the rats were used for subsequent experiments.

The RVSP and RVHI Declined in Rats After Intervention with MiR-135a Inhibitor

Statistical analysis was performed in accordance with the results of the PowerLab Biological Signal Collection and Processing System. The results showed that compared with the blank control group, the RVSP increased (>25 mmHg) in the model group, displaying a statistically significant difference (**p<0.01). However, the RVSP decreased markedly after intervention with miR-135a inhibitor compared with that of the model group ($^{\#\#}p$<0.01; Figure 1A). This suggested that miR-135a inhibitor could reduce RVSP in PAH rats. According to the records of RV and LV+S in rats of each group, RVHI was calculated. The results indicated that RVHI in the blank control group was remarkably lower than that of the model group (**p<0.01). Meanwhile, it decreased markedly in miR-135a inhibitor intervention group in comparison with the model group ($^{\#}p$<0.05; Figure 1B). The above results indicated that miR-135a inhibitor could reduce RVSP and RVHI in rats prominently.

Pathological Morphology of Rat Lung Tissues was Improved after Intervention with MiR-135a Inhibitor

HE staining of rat lung tissues in each group indicated that lung tissue cells were normal in morphology and were arranged closely in the blank control group. In the model group, the tunica media of the lung tissues were thickened evidently, and the cells were arranged loosely. Compared with the model group, the degree of vascular hypertrophy of lung tissues decreased markedly in the miR-135a inhibitor intervention group. Furthermore, the pathological damage was ameliorated prominently.

IL-6 and IL-1β Levels in Rat Lung Tissues were Down-Regulated after Intervention with MiR-135a Inhibitor

The expression levels of IL-6 in the supernatant of lung tissues were (4.88±0.51), (25.08±1.33) and (12.66±1.40) ng/L in the blank control group, model group and miR-135a inhibitor intervention group, respectively (Figure 3A). Statistical analysis indicated that the level of IL-6 in lung tissues was significantly elevated in the model group in comparison with the blank control group (**p<0.01). However, it was markedly declined after intervention with miR-135a inhibitor ($^{\#\#}p$<0.01). Subsequently, the level of IL-1β in rat lung tissues was detected as well. The results demonstrated that the level of IL-1β in lung tissues of the model group was evidently higher than that of the blank control group (**p<0.01). However, it decreased remarkably after interven-

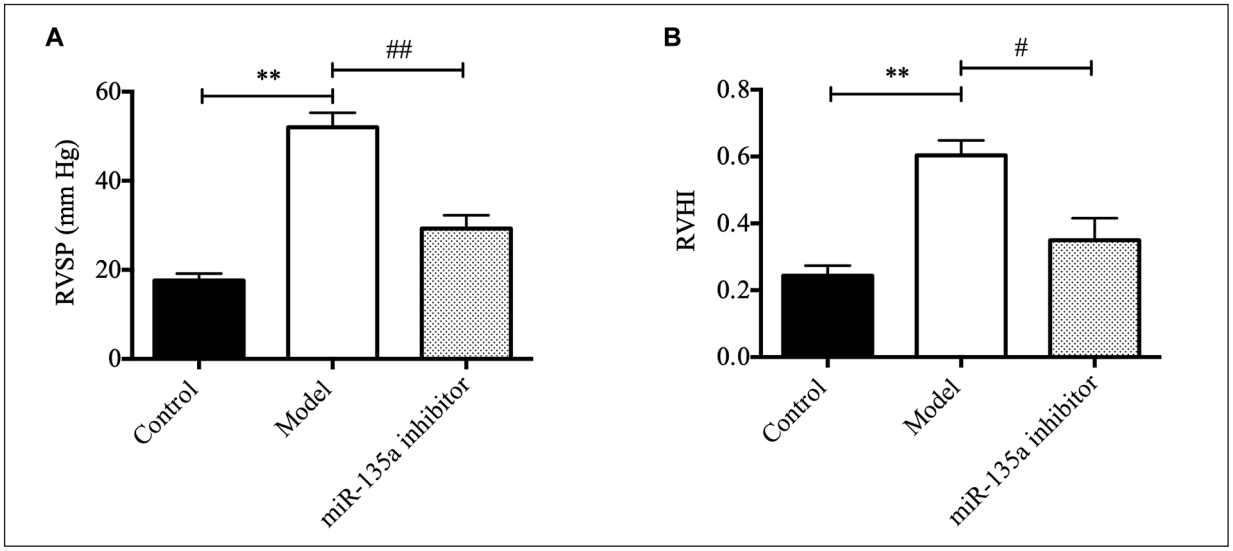

Figure 1. RVSP and RVHI of rats. **A,** RVSP of rats, **B,** RVHI of rats. (**p<0.01, $^{\#\#}p$<0.01, $^{\#}p$<0.05).

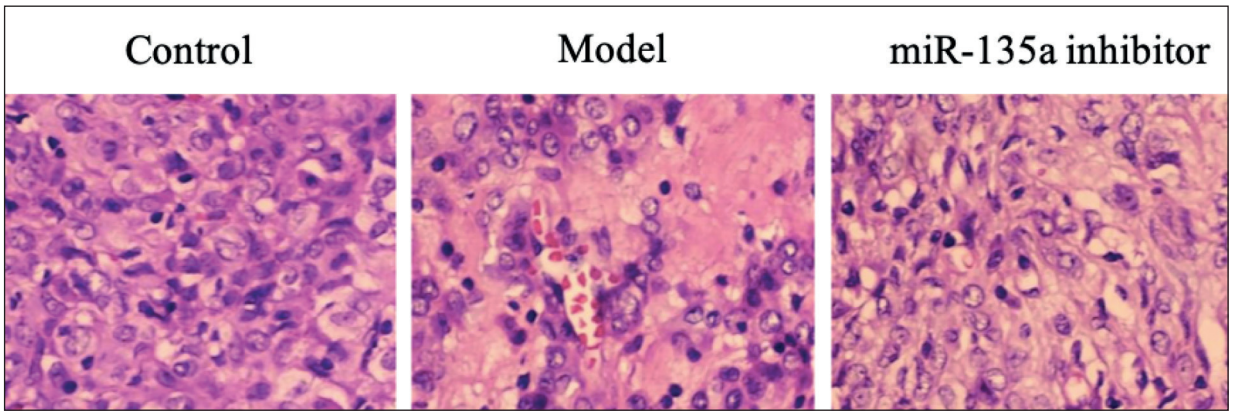

Figure 2. Changes in pathological morphology of rat lung tissues detected via HE staining (20×).

tion with miR-135a inhibitor ($^{\#}p<0.05$; Figure 3B). These results manifested that miR-135a inhibitor was capable of alleviating inflammatory response in the lung tissues of PAH rats.

The mRNA Levels of β-Catenin and GSK-3Ð in Rat Lung Tissues were Repressed after Intervention with MiR-135a Inhibitor

The changes in the mRNA levels of β-catenin and GSK-3β in the β-catenin/GSK-3β signaling pathway were detected by RT-PCR (Figure 4A). The results discovered that compared with the blank control group, the mRNA levels of β-catenin and GSK-3β in the lung tissues of the model group increased significantly (*$p<0.05$, **$p<0.01$). However, they decreased notably after intervention with miR-135a inhibitor ($^{\#}p<0.05$, $^{\#}p<0.05$; Figure 4B). The findings manifested that miR-135a inhibitor could suppress the activation of the β-catenin/GSK-3β signaling pathway at the transcription level.

The Protein Levels of β-Catenin and GSK-3β in Rat Lung Tissues were Repressed after Intervention with MiR-135a Inhibitor

To further explore the mechanism of miR-135a inhibitor in the rat model of PAH, the protein levels of β-catenin and GSK-3β in the β-catenin/GSK-3β signaling pathway were detected *via* Western blotting. The analysis of the optical

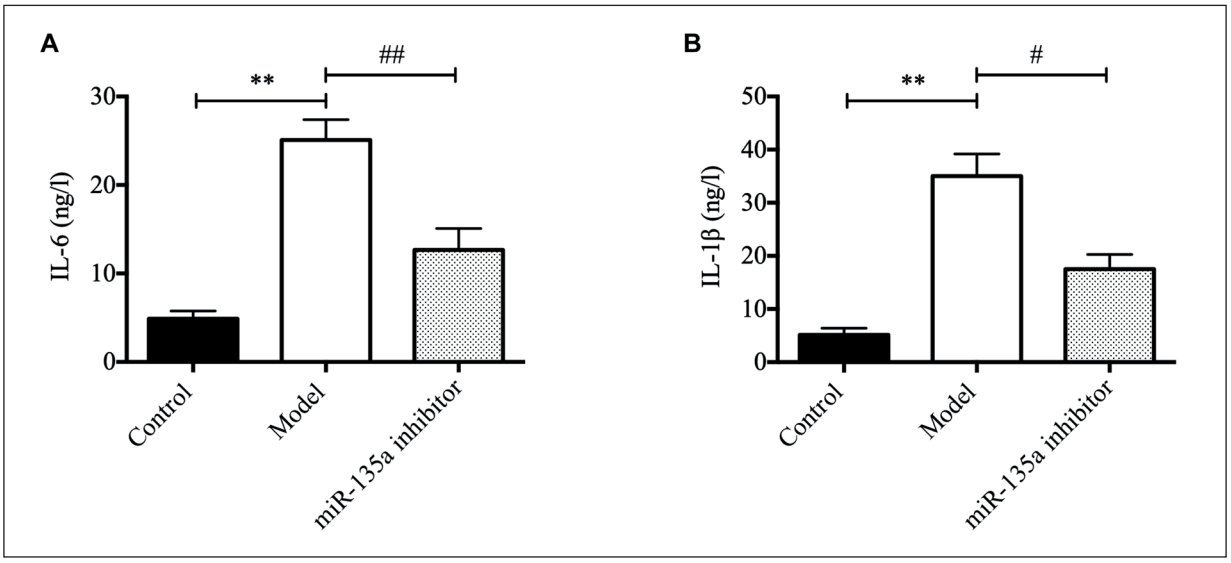

Figure 3. IL-6 and IL-1β levels in rat lung tissues. **A,** IL-6 level in rat lung tissues, **B,** IL-1β level in rat lung tissues. (**$p<0.01$, $^{\#\#}p<0.01$, $^{\#}p<0.05$).

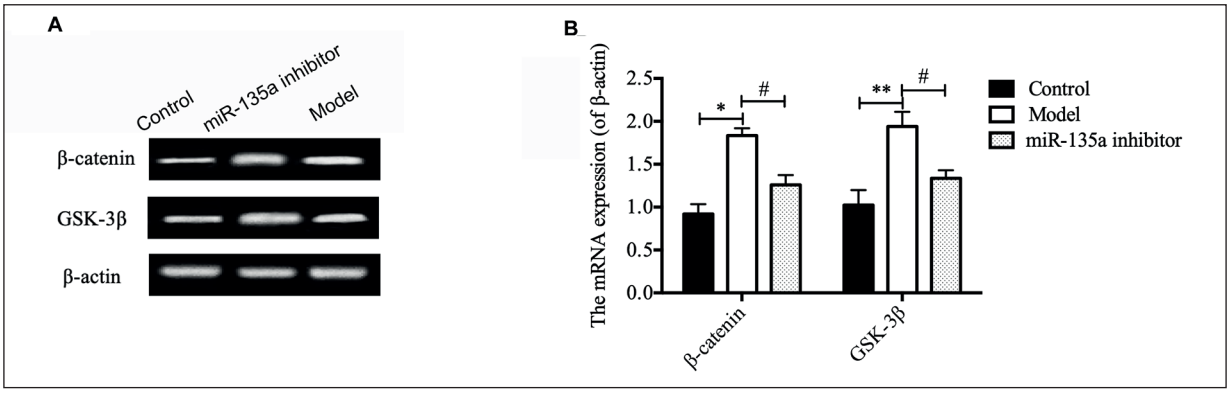

Figure 4. MRNA levels of β-catenin and GSK-3β**. A,** RT-PCR bands, with β-actin as the internal reference, **B,** Statistical charts of bands. ($^{**}p<0.05$, $^{\#\#}p<0.01$, $^{\#}p<0.05$).

density of bands (Figure 5A) revealed that the protein expression levels of β-catenin and GSK-3β were significantly up-regulated in the model group when compared with the blank control group ($^{*}p<0.05$, $^{*}p<0.05$). However, they were significantly down-regulated after intervention with miR-135a inhibitor ($^{\#\#}p<0.01$, $^{\#}p<0.05$; Figure 5B). The results indicated that miR-135a inhibitor might exert therapeutic effects on the rat model of PAH by repressing the β-catenin/GSK-3β signaling pathway.

Discussion

PAH is a chronic, progressive fibrotic lung disease characterized by intimal hyperplasia and remodeling of small pulmonary arteries. The primary pathological changes of PAH include collagen fiber deposition in lung tissues, hypertrophy and abnormal proliferation of pulmonary artery smooth muscle cells and pulmonary thrombosis[12]. However, the pathogenesis of PAH has not been fully elucidated. Generally, hypoxic pulmonary vasoconstriction, pulmonary vascular remodeling, pulmonary vascular endothelial dysfunction and autoimmune abnormality are accepted theories for PAH pathogenesis. Recently, researchers have discovered that the inflammatory response in PAH patients is abnormal. Hashimoto-Kataoka et al[13] have found that the expression of IL-6 is remarkably elevated in the serum of PAH patients. Meanwhile, the downstream target IL-21 is abnormally activated, further aggravating the inflammatory response. Lei et al[14] have indicated that the levels of serum IL-1β and TNF-α increase notably in PAH patients, while those of IL-10

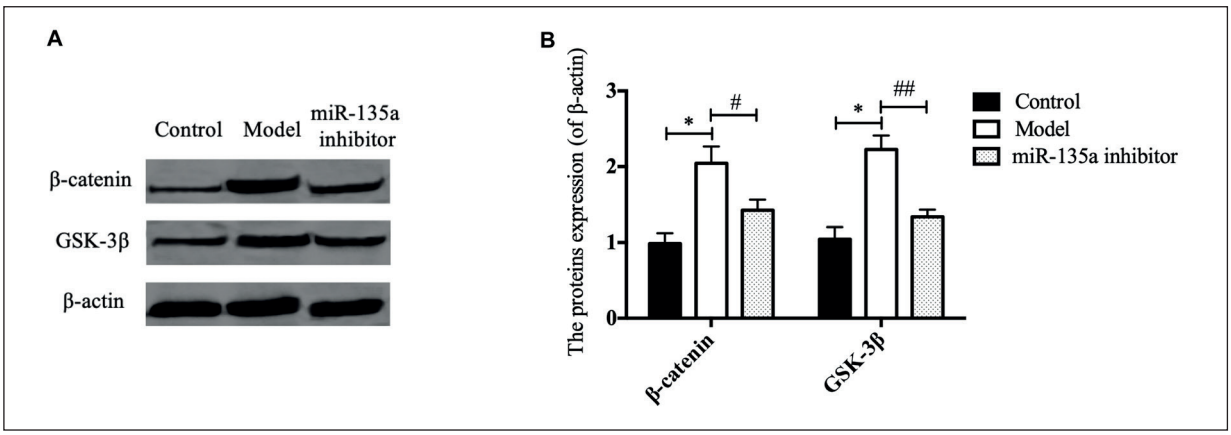

Figure 5. Protein levels of β-catenin and GSK-3β. **A,** Western blotting bands, with β-actin as the internal reference, **B,** Statistical charts of bands. ($^{**}p<0.05$, $^{\#\#}p<0.01$, $^{\#}p<0.05$).

and cGMP are markedly down-regulated. These findings indicate that abnormal inflammatory response plays a vital role in PAH.

As a multifunctional factor regulating cell activity, β-catenin is involved in various processes, including abnormal proliferation, differentiation and migration[15]. The expression level of β-catenin is positively correlated with the severity of pulmonary fibrosis. That is, highly expressed β-catenin indicates severe pulmonary fibrosis. Some studies have revealed that if the expression of β-catenin is suppressed by miRNA inhibitors, the production of myofibroblasts will be inhibited. This may eventually repress the occurrence of pulmonary fibrosis. GSK-3β, a downstream gene of β-catenin, plays crucial roles in embryogenesis and adult tissue homeostasis[16]. The β-catenin/GSK-3β signaling pathway exerts key effects on the oxidative stress response, inflammatory response and fibro-genic response. In particular, the pathway plays a crucial role in pulmonary fibrosis. Previous studies have indicated that inhibition on the activation of the β-catenin/GSK-3β signaling pathway can repress the occurrence and development of pulmonary fibrosis to a great extent. Silencing of GSK gene may lower or completely block the expression of fibronectin, thereby repressing the transformation of lung fibroblasts into myofibroblasts. For example, Cheng et al[17] have discovered that T helper 17 cells exert key effects on acute lung injury. The possible mechanism is associated with the activation of the Wnt/β-catenin signaling pathway. This implies that searching for targeted drugs capable of regulating β-catenin provides novel ideas for PAH treatment.

MiRNAs are short-chain small RNAs participating in the regulation of the transcription or translation of target genes or proteins. In recent years, the relationship between miRNAs and diseases has become a hotspot of research in the medical field. For example, miR-135a has been found to be involved in multiple biological processes in the body. It mediates the occurrence and development of various diseases, such as coronary heart disease, hypertension and tumors[18,19]. Lee et al[20] have discovered that abnormal expression of miRNAs can induce the occurrence and development of PAH. However, few papers have elucidated the relationship between miR-135a and PAH.

In this report, the rat model of PAH was successfully established *via* intraperitoneal injection of MCT. The results revealed that compared with the model group, the pathological damage to lung tissues of rats was ameliorated prominently, and RVSP and RVHI declined remarkably after treatment with the miR-135a inhibitor. Meanwhile, the release of inflammatory factors was significantly reduced. To further explore the regulatory mechanism, the mRNA and protein expressions of β-catenin and GSK-3β in the β-catenin/GSK-3β signaling pathway were detected. Quantitative Real Time-Polymerase Chain Reaction (QRT-PCR) and Western blotting showed that the mRNA and protein expressions of β-catenin and GSK-3β were both significantly down-regulated after the intervention with miR-135a inhibitor. Our findings indicated that miR-135a inhibitor exerted its therapeutic effects on the rat model of PAH by inhibiting the β-catenin/GSK-3β signaling pathway.

Conclusions

We found that miR-135a inhibitor can significantly alleviate inflammatory response in lung tissues and ameliorate damage to the pathological morphology. The possible underlying mechanism may be associated with the β-catenin/GSK-3β signaling pathway.

Conflict of Interest

The Authors declare that they have no conflict of interests.

References

1) Matsubara H, Ogawa A. Treatment of idiopathic/hereditary pulmonary arterial hypertension. J Cardiol 2014; 64: 243-249.
2) Li WJ, Hu K, Yang JP, Xu XY, Li N, Wen ZP, Wang H. HMGB1 affects the development of pulmonary arterial hypertension via RAGE. Eur Rev Med Pharmacol Sci 2017; 21: 3950-3958.
3) Keating GM. Macitentan: a review in pulmonary arterial hypertension. Am J Cardiovasc Drugs 2016; 16: 453-460.
4) Girerd B, Lau E, Montani D, Humbert M. Genetics of pulmonary hypertension in the clinic. Curr Opin Pulm Med 2017; 23: 386-391.
5) Humbert M, Montani D, Evgenov OV, Simonneau G. Definition and classification of pulmonary hypertension. Handb Exp Pharmacol 2013; 218: 3-29.
6) Dunach M, Del VB, Garcia DHA. p120-catenin in canonical Wnt signaling. Crit Rev Biochem Mol Biol 2017; 52: 327-339.

7) Duan P, Bonewald LF. The role of the wnt/beta-catenin signaling pathway in formation and maintenance of bone and teeth. Int J Biochem Cell Biol 2016; 77: 23-29.

8) Vilchez V, Turcios L, Marti F, Gedaly R. Targeting Wnt/beta-catenin pathway in hepatocellular carcinoma treatment. World J Gastroenterol 2016; 22: 823-832.

9) Bahrami A, Amerizadeh F, ShahidSales S, Khazaei M, Ghayour-Mobarhan M, Sadeghnia HR, Maftouh M, Hassanian SM, Avan A. Therapeutic potential of targeting Wnt/beta-catenin pathway in treatment of colorectal cancer: rational and progress. J Cell Biochem 2017; 118: 1979-1983.

10) Gao F, Liu P, Narayanan J, Yang M, Fish BL, Liu Y, Liang M, Jacobs ER, Medhora M. Changes in miRNA in the lung and whole blood after whole thorax irradiation in rats. Sci Rep 2017; 7: 44132.

11) Li Q, Wang J, Zhu X, Zeng Z, Wu X, Xu Y, Xie J, Yu J. Dihydromyricetin prevents monocrotaline-induced pulmonary arterial hypertension in rats. Biomed Pharmacother 2017; 96: 825-833.

12) Harbaum L, Renk E, Yousef S, Glatzel A, Luneburg N, Hennigs JK, Oqueka T, Baumann HJ, Atanackovic D, Grunig E, Boger RH, Bokemeyer C, Klose H. Acute effects of exercise on the inflammatory state in patients with idiopathic pulmonary arterial hypertension. BMC Pulm Med 2016; 16: 145.

13) Hashimoto-Kataoka T, Hosen N, Sonobe T, Arita Y, Yasui T, Masaki T, Minami M, Inagaki T, Miyagawa S, Sawa Y, Murakami M, Kumanogoh A, Yamauchi-Takihara K, Okumura M, Kishimoto T, Komuro I, Shirai M, Sakata Y, Nakaoka Y. Interleukin-6/interleukin-21 signaling axis is critical in the pathogenesis of pulmonary arterial hypertension. Proc Natl Acad Sci U S A 2015; 112: E2677-E2686.

14) Lei Y, Zhen J, Ming XL, Jian HK. Induction of higher expression of IL-beta and TNF-alpha, lower expression of IL-10 and cyclic guanosine monophosphate by pulmonary arterial hypertension following cardiopulmonary bypass. Asian J Surg 2002; 25: 203-208.

15) Qu Z, Su F, Qi X, Sun J, Wang H, Qiao Z, Zhao H, Zhu Y. Wnt/beta-catenin signalling pathway mediated aberrant hippocampal neurogenesis in kainic acid-induced epilepsy. Cell Biochem Funct 2017; 35: 472-476.

16) Kim W, Kim M, Jho EH. Wnt/beta-catenin signalling: from plasma membrane to nucleus. Biochem J 2013; 450: 9-21.

17) Cheng L, Zhao Y, Qi D, Li W, Wang D. Wnt/beta-catenin pathway promotes acute lung injury induced by LPS through driving the Th17 response in mice. Biochem Biophys Res Commun 2018; 495: 1890-1895.

18) Li D, Deng T, Li H, Li Y. MiR-143 and miR-135 inhibitors treatment induces skeletal myogenic differentiation of human adult dental pulp stem cells. Arch Oral Biol 2015; 60: 1613-1617.

19) Honardoost M, Arefian E, Soleimani M, Soudi S, Sarookhani MR. Development of insulin resistance through induction of miRNA-135 in C2C12 Cells. Cell J 2016; 18: 353-361.

20) Lee A, McLean D, Choi J, Kang H, Chang W, Kim J. Therapeutic implications of microRNAs in pulmonary arterial hypertension. BMB Rep 2014; 47: 311-317.